Attractor Selection in Chaotic Dynamics

R. Meucci,[1] E. Allaria,[2,1] F. Salvadori,[2,1] and F. T. Arecchi[2,1]
[1]*Istituto Nazionale di Ottica Applicata, Largo E. Fermi, 5 50125 Firenze, Italy*
[2]*Department of Physics, Università di Firenze, Italy*
(Received 4 April 2005; revised manuscript received 17 June 2005; published 26 October 2005)

For different settings of a control parameter, a chaotic system can go from a region with two separate stable attractors (generalized bistability) to a crisis where a chaotic attractor expands, colliding with an unstable orbit. In the bistable regime jumps between independent attractors are mediated by external perturbations; above the crisis, the dynamics includes visits to regions formerly belonging to the unstable orbits and this appears as random bursts of amplitude jumps. We introduce a control method which suppresses the jumps in both cases by filtering the specific frequency content of one of the two dynamical objects. The method is tested both in a model and in a real experiment with a CO_2 laser.

DOI: 10.1103/PhysRevLett.95.184101 PACS numbers: 05.45.Gg, 42.65.Pc

By tuning a control parameter, a chaotic system can either display two attractors (generalized bistability) [1–3] or exhibit an interior crisis [4,5], whereby a chaotic attractor suddenly expands including the region of an unstable orbit. In the former case, starting from an assigned initial condition, the system remains on one attractor, and only external perturbations can induce jumps between the two attractors; the relative weight of the two attractors is given by the size ratio of the two domains of the initial conditions leading to either one. In the latter case, whatever the initial condition, the system visits the whole phase space of the two dynamical objects, even though for different amounts of time; any initial condition generates the trajectory visiting the whole single attractor; however, a memory of the previously separeted regions remains and the fractional time η spent on the formerly unstable orbit results in bursts of anomalous amplitude signal (crisis-induced intermittency [6]).

In the bistable case [7], we show how a single attractor selection is performed by a feedback including a frequency filter, based on the different spectral content of the two attractors; then we demonstrate that the selection method is still effective beyond the crisis. In this latter case, the selection eliminates the anomalous bursts, thus regularizing the output signal. The method leaves unperturbed the chaotic features of the selected attractor, thus it should not be confused with chaos control [8] which stabilizes one of the unstable periodic orbits within a single attractor.

We apply these general considerations to a periodically driven CO_2 laser [2]. The attractor selection is realized by adding to the loss modulator of the CO_2 laser a feedback loop including a frequency filter, which modifies the driving signal, quenching or enhancing some specific frequency components, depending on the feedback sign.

The laboratory setup is shown in Fig. 1.

It consists of a single-mode CO_2 laser with an intracavity electro-optic loss modulator (EOM). The cavity length is $L = 1.42$ m and the total transmission T is about 0.10 for a single pass. The intensity decay rate can be expressed as

$$k(t) = k\{1 + \alpha \sin^2[B_0 + F_{\mathrm{mod}}(t)]\} \qquad (1)$$

where $k = cT/L$, c being the speed of light in the vacuum, $\alpha = (1 - 2T)/2T$, B_0 is a bias voltage, and $F_{\mathrm{mod}}(t)$ is the modulation applied to the EOM.

We consider a sinusoidal modulation $F_{\mathrm{mod}}(t) = A \sin(2\pi f t)$ where $f = 100$ kHz is about twice the relaxation frequency of the laser [2]. The modulation signal is provided by a waveform generator (WG). The laser is pumped by a dc discharge current stabilized at 8.00 mA, while the threshold current is 6.50 mA. The filter NF

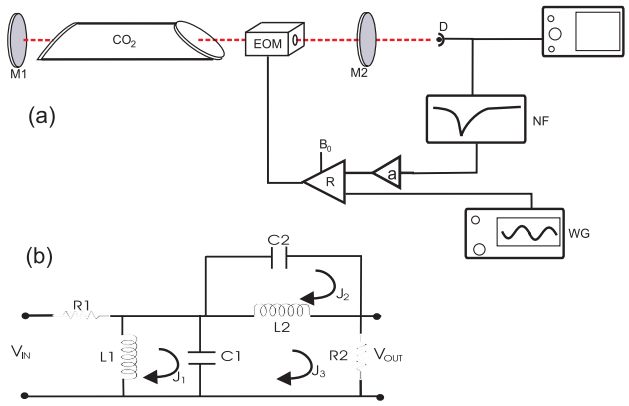

FIG. 1 (color online). (a) Laboratory setup consisting of a CO_2 laser with loss modulation, partly due to an external driving and partly due to a feedback loop including the filter. EOM, electro-optic modulator; $M1$, $M2$, mirrors; D, detector; NF, notch filter; a, amplifier for the filter signal; R, differential amplifier; B_0, bias voltage and WG, wave generator. (b) Electronic scheme of the passive filter (NF). The component values for the filter are $R_1 = 600\ \Omega$, $R_2 = 20\ \mathrm{k}\Omega$, $L_1 = 1.44$ mH, $L_2 = 17$ mH, $C_1 = 19$ nF, and $C_2 = 560$ pF.

[Fig. 1(b)] has a notch frequency given by $f_{\text{notch}} = 1/(2\pi\sqrt{L_2C_2})$; its input is the laser intensity and its output is amplified by a.

Increasing the modulation amplitude A [see Fig. 2(a)], the system undergoes a sequence of subharmonic bifurcations leading to a small amplitude chaotic attractor. Further increase of A (above 1.2 V) induces the occurrence of a regime where bursts of high-amplitude orbits of period three and period four ($P3$ and $P4$) are intercalated with the small amplitude chaotic attractor [Figs. 2(b) and 2(c)].

Bursting events follow a statistical law typical of Type I intermittency [9]. Plotting the counts of the interbursting times τ, we obtain experimentally, and confirm numerically, exponential decay of the burst occurrence versus the interbursting time, with an experimental mean separation $\langle\tau_{\text{exp}}\rangle = (0.366 \pm 0.001)$ ms; in the numerical case we find $\langle\tau_{\text{num}}\rangle = (1.04 \pm 0.05)$ ms. The quantitative difference is due to the fact that the numerical noise is much smaller than the laboratory noise.

The modulated CO_2 laser has been initially modeled by two coupled rate equations, for the laser intensity and the population inversion [2]. However, for a good agreement between model and experimental data, one must account for long time interactions of the resonant molecular transition with other molecular levels. It is then convenient to add three further linear equations, using a model of five differential equations. The rescaled equations for the modulated laser were reported in Ref. [10]; the new parameter values that fit the present experimental situation are $k_0 = 30$, $\alpha = 4$, $B_0 = 0.1794$, $\Gamma_1 = 10.0643$, $\Gamma_2 = 1.0643$, $P_0 = 0.01987$, $\gamma = 0.05$, and $z = 10$. The threshold for P_0 is 0.0164.

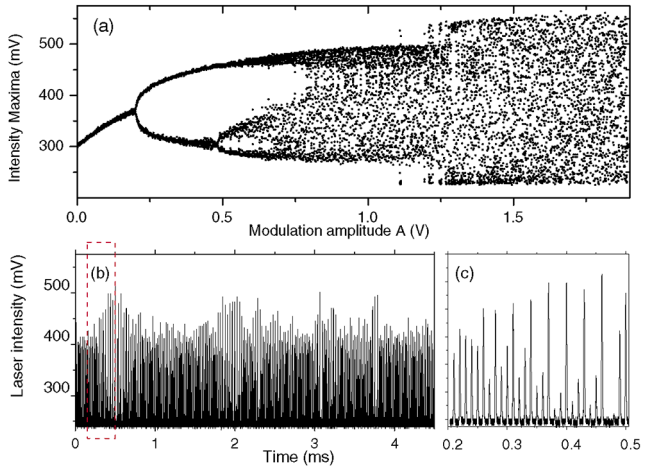

FIG. 2 (color online). Experimental data. (a) Stroboscopic bifurcation diagram of the unperturbed system as a function of the modulation amplitude A; the discontinuity around 1.2 V corresponds to the sudden onset of the interior crisis. (b) Time evolution of the laser output intensity in the bursting regime. (c) Zoom of (b) corresponding to the dashed box; it provides evidence of $P3$ and $P4$ oscillations.

We report in Figs. 3(a) and 3(b) the numerical bifurcation diagrams for two different initial conditions. Figure 3(a) shows the subharmonic cascade corresponding to the experimental data of Fig. 2; it starts precisely at $A = 0.05$ with $P2$ and continues with the chaotic window at $A = 0.065$; at $A \simeq 0.102$ the attractor displays a sudden increase corresponding to a crisis; from there, it merges with the "ghost" of the unstable $P3$ and hence yields the bursts observed in Fig. 2. Figure 3(b) displays a $P3$ attractor born from a saddle-node bifurcation at $A = 0.055$ and disappearing by boundary crisis [4] at $A = 0.07$, for an initial condition $x_1(0) = 0.43 \times 10^{-1}$. Figure 3(c) shows the stability regimes of $P3$ for a set of different initial conditions; the fact that $P3$ is born and dies at different control parameters is a demonstration of (i) the nestedness of the basin boundaries between the $P3$ and the subharmonic attractors and (ii) the fragility of the $P3$ attractor with respect to the subharmonic one.

The bistable interval around $A = 0.06$ is characterized by two different frequency contents of the $P3$ and subharmonic attractor; based on this difference we adjust the feedback filter in order to enhance or depress the $f/3$ component. This way, we select either one of the two attractors of the bistable regime, as shown in Figs. 4(a) and 4(b).

Above $A = 0.1$ an interior crisis expands the chaotic attractor into the region of the unstable $P3$, thus giving rise to a new attractor region which can be still discriminated by its frequency content. If we want to quench this

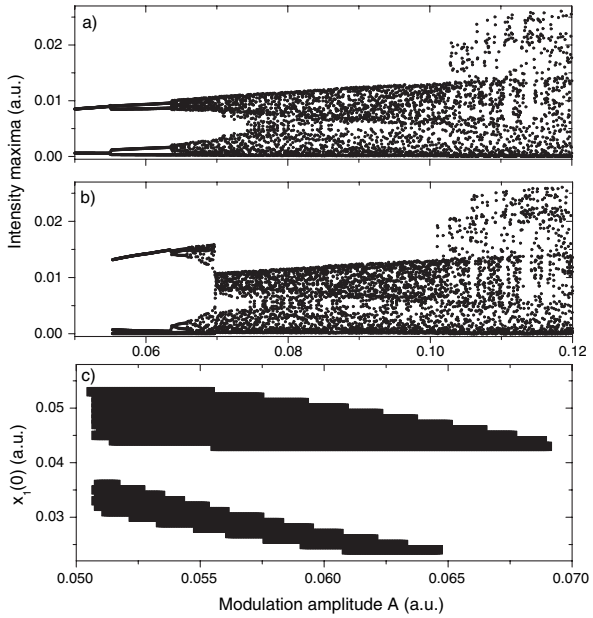

FIG. 3. (a) and (b) Numerical bifurcation diagrams obtained starting from two different initial conditions. (a) $x_1(0) = 0.43 \times 10^{-3}$ (b) $x_1(0) = 0.43 \times 10^{-1}$. The bistable range is $A \in (0.05, 0.07)$ while bursting regime is occurring after $A = 0.1$. (c) Parameter regions of stable existence of $P3$ for different initial conditions.

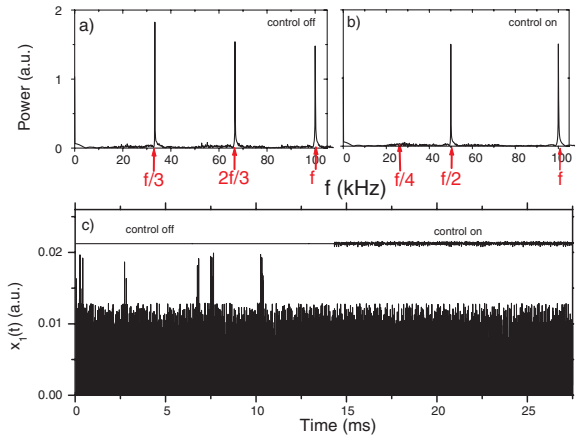

FIG. 4 (color online). (a) Numerical power spectrum corresponding to the attractor at $A = 0.06$ and to the initial condition in Fig. 3(b). (b) Selection of the other attractor after the control. (c) Numerical simulation of the time dependence of the laser intensity x_1 for $A = 0.105$ (beyond crisis). The control is applied at $t = 7$ ms. The upper trace represents the control signal for $G = 2.1\%$, on the same amplitude scale as x_1. Similar results can be obtained by applying the perturbation to the pump parameter P_0.

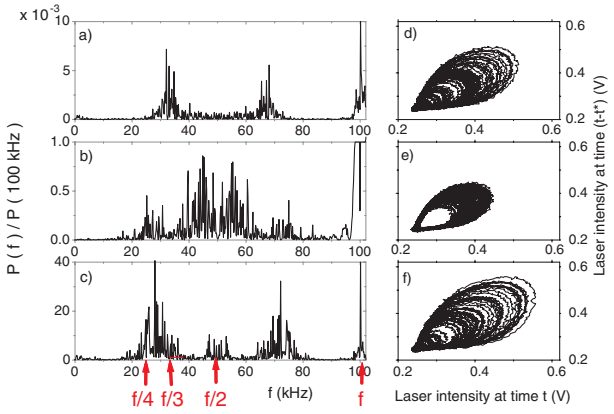

FIG. 5 (color online). Experimental frequency spectra of the laser intensity (a) in the busrting regime, (b) with negative feedback, showing depression at $f/3$ and $f/4$ components, (c) with positive feedback showing enhancement at $f/3$ and $f/4$ components. Notice the different vertical scales; indeed the amount of $f/4$ in (c) is 40 times larger than in (b). On the right, corresponding experimental attractors, reconstructed by an embedding technique, showing, respectively, (d) coexistence of both attractors, (e) elimination of the large attractor, (f) enhancement of the large attractor.

region, we send its main frequency components ($P3$ and $P4$) as a negative feedback signal via the frequency filter. If on the contrary we change the feedback sign, we enhance the role of this region against the rest of the attractor.

The frequency components corresponding to the subharmonic attractor are slightly affected by the filter (NF) whose notch frequency is selected at the first subharmonic $f/2$, that is, 50 kHz. The filter is ac coupled, so that the low frequency components, which control the long time dynamics, are not affected. The notch filter used in the experiment was already introduced in Refs. [11,12].

The filter output is amplified and sent to the negative or positive input of the differential amplifier (R). When the control is inserted, the modulation $F_{\mathrm{mod}}(t)$ is perturbed by aV_{out}, where V_{out} and a are the output of the filter and its amplification, respectively. We define the coupling strength G as the ratio aV_{out}/A between the perturbation and the modulation amplitude A. Figure 4(c) shows the bursting regime beyond crisis and its suppression when the perturbation is $G \simeq 2\%$.

In Fig. 5 we report the experimental data at $A = 1.25$ V, for the uncontrolled dynamics 5(a) and 5(d) and the for the controlled one, both with negative 5(b) and 5(e) and positive 5(c) and 5(f) feedback. On the left we plot the frequency spectra and on the right the corresponding attractors, reconstructed by the embedding technique. The larger amplitude chaotic attractor is drastically reduced in 5(b) and 5(e) giving evidence of burst suppression; on the contrary, it is enhanced for a positive feedback in 5(c) and 5(f).

A quantitative evidence of suppression of the large amplitude bursts is provided by the fractional time indicator η which is measured by

$$\eta = \frac{(\sum_k T_{Bk})}{T}, \tag{2}$$

T being the duration of the recorded time series and $\sum_k T_{Bk}$ the total duration of burst events within T.

The bursts are detected by selecting a threshold in order to distinguish the large amplitude spikes from the small amplitude chaotic dynamics. The behavior of η from the noncontrolled to the controlled regime is reported in Fig. 6 as a function of the coupling strength G. The transition toward complete control ($\eta = 0$) is characterized by a power law with an exponent $-1/2$,

$$\eta \propto |G - G_c|^{-1/2}. \tag{3}$$

Such a behavior, confirmed also by numerical simulations, indicates the presence of a phase transition of type I intermittency. The estimated value for the exponential decay of η as a function of $G - G_c$ is in agreement with the theoretical predictions for this transition [9,13]. A similar feature has also been reported in the transition to phase synchronization of homoclinic chaos with periodic perturbation [14]. Very close to complete control, numerical and experimental data deviate from the power law.

The perturbation can be applied to other control parameters instead of the cavity losses. For example, it can be added to the pump parameter P_0; in this case, control of

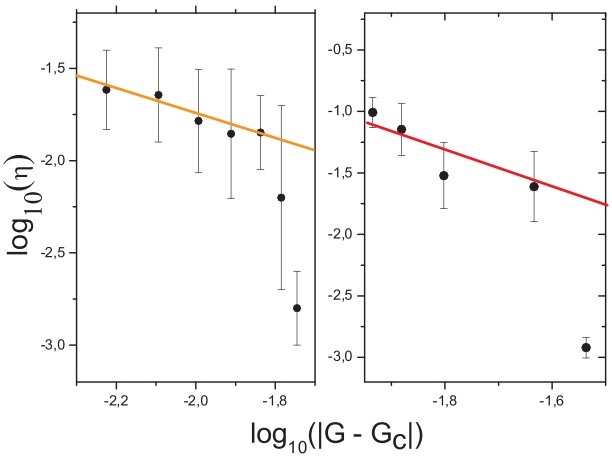

FIG. 6 (color online). Numerical (left) and experimental (right) evidence of the power law dependence η on G. The straight lines have slope $-1/2$. Modeling this transition as $\eta \propto |G - G_c|^{-1/2}$, the critical parameter G_c is estimated from the fit as $G_c = 0.00244$ in the numerical case and $G_c = 0.0112$ in the experimental case.

bursting is achieved for a relative perturbation of the order of $G \simeq 0.05\%$.

Epidemic outbreaks offer another example of bursting phenomena. Recently an epidemic model called SEIR [15] has been shown to be ruled by the same equations as the CO_2 laser. The SEIR term refers to the population dynamics of individuals distributed over different states, namely, susceptible (S), exposed (E), infectious (I), and recovered (R); here the key nonlinearity is the SI product. In laser dynamics I and S are replaced by the photon number and population inversion, respectively, and their product provides the fundamental nonlinearity [16]. Controlling through the pump modulation is equivalent, in the SEIR model, to controlling through the birth rate modulation, whereas controlling through cavity losses corresponds to modulating the recovery rate, which is in fact not possible in nature [16].

In summary, we have experimentally demonstrated that a suitable linear filtering can suppress bursting in chaotic dynamics systems with occasional amplitude jumps, once the frequency components of the bursting regimes have been isolated. This control method has a wide applicability; the analogy with the epidemiological SEIR model suggests a possible application to epidemic outbreaks, as an alternative to an adaptive scheme recently introduced [17].

Work is partly supported by FIRB Contract No. RBAU01B49F_002.

[1] F. T. Arecchi and F. Lisi, Phys. Rev. Lett. **49**, 94 (1982); **50**, 1330 (1983).
[2] F. T. Arecchi, R. Meucci, G. Puccioni, and J. R. Tredicce, Phys. Rev. Lett. **49**, 1217 (1982).
[3] J. M. Saucedo-Solorio *et al.*, J. Opt. Soc. Am. B **20**, 490 (2003).
[4] C. Grebogi, E. Ott, and J. Yorke, Phys. Rev. Lett. **48**, 1507 (1982).
[5] D. Dangoisse, P. Glorieux, and D. Hennequin, Phys. Rev. Lett. **57**, 2657 (1986).
[6] C. Grebogi, E. Ott, and J. Yorke, Physica (Amsterdam) **7D**, 181 (1983).
[7] The different spectral content is crucial for the validity of the proposed method, which then does not hold in case of complete mirror symmetry of the two attractors as, e.g., in the forced Duffing oscillator of Ref. [1].
[8] E. Ott, C. Grebogi, and J. Yorke, Phys. Rev. Lett. **64**, 1196 (1990). For a comprehensive review on this subject see S. Boccaletti, C. Grebogi, Y. C. Lai, H. Mancini, and D. Maza, Phys. Rep. **329**, 103 (2000), and references therein.
[9] Edward Ott, in *Chaos in Dynamical Systems* (Cambridge University Press, Cambridge, England, 1994), pp. 279–280.
[10] R. Meucci, D. Cinotti, E. Allaria, L. Billings, I. Triandaf, D. Morgan, and I. B. Schwartz, Physica (Amsterdam) **189D**, 70 (2004).
[11] R. A. Tesi, E. H. Abed, R. Genesio, and H. O. Wang, Automatica **32**, 1255 (1996).
[12] R. Meucci, M. Ciofini, and R. Abbate, Phys. Rev. E **53**, R5537 (1996).
[13] P. Manneville and Y. Pomeau, Physica (Amsterdam) **1D**, 219 (1980).
[14] S. Boccaletti, E. Allaria, R. Meucci, and F. T. Arecchi, Phys. Rev. Lett. **89**, 194101 (2002).
[15] L. Billings, E. Bollt, D. Morgan, and Ira B. Schwartz, in *Proceedings of the Fourth International Conference on Dynamical Systems and Differential Equations*, (American Institute for Mathematical Sciences, Wilmington, NC, USA, 2002), p. 122.
[16] Min-Young Kim, R. Roy, J. L. Aron, T. W. Carr, and Ira B. Schwartz, Phys. Rev. Lett. **94**, 088101 (2005).
[17] I. B. Schwartz, L. Billings, and E. M. Bollt, Phys. Rev. E **70**, 046220 (2004).